Journal of Materials Physics and Chemistry, 2014, Vol. 2, No. 1, 1-8
Available online at http://pubs.sciepub.com/jmpc/2/1/1

DOI:10.12691/jmpc-2-1-1

Characterization of Cellulose Nanocrystals Produced by Acid-Hydrolysis from Sugarcane Bagasse as Agro-Waste

Anuj Kumar[1], Yuvraj Singh Negi[1,*], Veena Choudhary[2], Nishi Kant Bhardwaj[3]

[1]Department of Polymer and Process Engineering, Indian Institute of Technology Roorkee, India
[2]Centre for Polymer Science and Engineering, Indian Institute of Technology Delhi, India
[3]Thapar Centre for Industrial Research and Development, Yamuna Nagar, Haryana, India
*Corresponding author: yuvrajnegi@gmail.com

Received November 09, 2013; Revised December 10, 2013; Accepted December 30, 2013

Abstract Sugarcane bagasse (SCB) is abundantly available agro-waste world-wide and has been used in different applications and its utilization as a source of cellulose attracting attention in the area of biomedical and other applications. The present study investigates the surface morphology, topography, structural, elemental and thermal properties of cellulose nanocrystals (CNCs) extracted by acid-hydrolysis from sugarcane bagasse as agro-waste. Morphological (field emission scanning electron microscopy (FE-SEM), atomic force microscopy (AFM), transmission electron microscopy (TEM)), structural (fourier transformed infrared (FTIR) spectroscopy, X-ray diffraction (XRD)), elemental analysis (energy dispersive x-ray diffraction (EDX)) and thermal characterization (TG-DTG-DTA) of CNCs was carried out. Morphological characterization clearly showed the formation of rod-shaped CNCs having size in the range of 250-480 nm (length) and 20-60 nm (diameter). Elemental analysis (EDX) showed 0.72 wt% sulfur impurity in CNCs along with other main components. X-ray diffraction and thermal analysis revealed that CNCs have higher crystallinity (72.5%) than that of chemically purified cellulose (CPC) (63.5%) but have lower thermal stability. These lab extracted CNCs supposed to have a high potential as nano-reinforcement into bionanocomposite for biomedical and other value-added products in industrial applications.

Keywords: *sugarcane bagasse, cellulose nanocrystals, acid-hydrolysis, nanotechnology, agro-waste*

Cite This Article: Anuj Kumar, Yuvraj Singh Negi, Veena Choudhary, and Nishi Kant Bhardwaj, "Characterization of Cellulose Nanocrystals Produced by Acid-Hydrolysis from Sugarcane Bagasse as Agro-Waste." *Journal of Materials Physics and Chemistry* 2, no. 1 (2014): 1-8. doi: 10.12691/jmpc-2-1-1.

1. Introduction

Cellulose-based Nanomaterials a sustainable and renewable material (however living sources from which they are extracted are sustainable and renewable, not the natural fibres or nanoparticles [1] have been of increasing interest as potential nano-reinforcing filler into biocomposites for industrial and biomedical applications. They have low density, high aspect ratio, good mechanical properties, low thermal expansion, low toxicity, surfaces having hydroxyl groups (-OH) that can be readily chemically functionalized [2-9]. These nanomaterials have been extensively studied for a wide variety of potential applications such as nanofillers for polymer nanocomposites, protective coatings, barrier/separation membranes and filtration systems, scaffolds for tissue engineering, transparent films, antimicrobial films, pharmaceuticals, drug delivery, organic solar cells, supercapacitors, substrates for flexible electronics, and lithium-ion batteries etc. [6,10].

Two general classes of cellulose nanomaterials (CNs) that can be extracted from different resources such as plant, animal, or mineral plants are cellulose nanocrystals (CNCs) and cellulose nanofibrils (CNFs). Cellulose nanocrystals can be referred as cellulose nanowhiskers (CNW) or nanocrystalline cellulose (NCC) [11,12] while cellulose nanofibrils can be referred as nanofibrillated cellulose (NFC), or microfibrillated cellulose (MFC) depending on their size and extraction method [13]. CNCs are needle-like cellulose particles having at least one dimension equal or less than 100 nm with highly crystalline nature.

However, in recent times, plants based cellulose has been extensively exploited for the production of this nano-crystalline material [14]. Cellulose is a natural hydrophilic polymer composed of β-1,4-linked anhydro-D-glucose units and having hydroxyl (-OH) groups that enable cellulose to establish strong hydrogen bonds. Major sources of cellulose are wood, cotton, hemp, flax, sisal, sugarcane bagasse, corncob, cassava bagasse, banana rachis, soy hulls, mengkuang leaves (Pandanus tectorius), Phormium tenax leaf fibres, rice husk and jute etc. [11,15-23]. Other major components are hemicelluloses, and lignin into natural fibres. Lignin is like as cementing-matrix for cellulose and hemicellulose having linkages of two types: (1) Ester-type bond which is sensitive to alkali solutions. (2) Ether-type bond which is insensitive to alkali solutions. Cellulose is a semi-crystalline polymer while hemicellulose and lignin are amorphous polymers [19,24]. Plant cellulose comprises of a hierarchical composite structure of nano-scale networked fibrils. This semi-crystalline composite structure has amorphous and

crystalline regions in varying proportions depending on the plant species. For this reason, the characteristics of nano-cellulosic materials, particularly chemical compositions and dimensions, depend largely on particular plants, their origin, and extraction methods [16,25,26]. Various extraction processes have been used for the production of CNCs but acid-hydrolysis (H_2SO_4) is the most well-known, efficient, and widely used extraction method. Under controlled conditions, this process allows to break and removal of disordered and amorphous regions of cellulosic fibres, releasing single and well defined crystals in the form of CNCs [5,27]. It has been observed that the performance of CNCs as a nano-reinforcing agent influenced with the variation of morphology and properties of these nanoparticles which depend mainly on original source of cellulose and extraction methods [6,16,28]. Therefore, extensive characterization of CNCs from different sources is very crucial for the development of bionanocomposites.

Although the production of CNCs has been investigated extensively in the papers from a variety of natural fibres sources in detail, the use of sugarcane bagasse (as agro-waste available in large quantities world-wide) as a natural fibres source for the production of CNCs has not been widely exploited yet for reinforcing agent in bionanocomposites. In previous studies, few approaches have been reported for the extraction of CNCs from sugarcane bagasse as agro-waste, such as high pressure homogenization [29], acid-hydrolysis [30,31,32,33], alkaline hydrolysis followed by acid-hydrolysis [34] but it requires extensive study in extraction and characterization of CNCs from this waste materials and utilization for value-added products.

The objective of this present work was to extract CNCs from sugarcane bagasse by acid hydrolysis (H_2SO_4) having high crystallinity index, supposed to have good thermal stability, and surface morphology (shape and size) suitable for use as reinforcing agent in the fabrication of bionanocomposites for different applications. The CNCs obtained were characterized for surface topography and morphology by FE-SEM, AFM, and TEM, chemical and physical and elemental characterization by FTIR spectroscopy, XRD, EDX and thermal properties by thermogravimetric analysis (TG, DTG, and DTA). Image analysis of the extracted product was also done using ImageJ software to investigate the length and diameter of the CNCs.

2. Materials and Methods

2.1. Materials

Sugarcane bagasse (agro-waste) was provided by a local sugar factory (Uttar Pradesh, India). After drying in sunlight, it was ground and sieved under 30 mesh sieves. Bagasse was dried in oven at 105°C for 3 h and stored at room temperature in air tight polybag. Benzene, methanol, sodium chlorite, acetic acid, sodium hydroxide, potassium hydroxide, sulfuric acid, cellulose dialysis membrane (tubes) were of analytical grade. Distilled water (DW) was used throughout the experiments.

2.2. Methods

2.2.1. Isolation of Chemically Purified Cellulose

Chemically purified cellulose (CPC) from sugarcane bagasse (SCB) was isolated according to the previously reported methods [35,36,37] as referred elsewhere [19] and shown in Figure 1 (a). Finally the, product was dried in air-circulated oven at 105°C for 6 h followed by storage in air tight polybags.

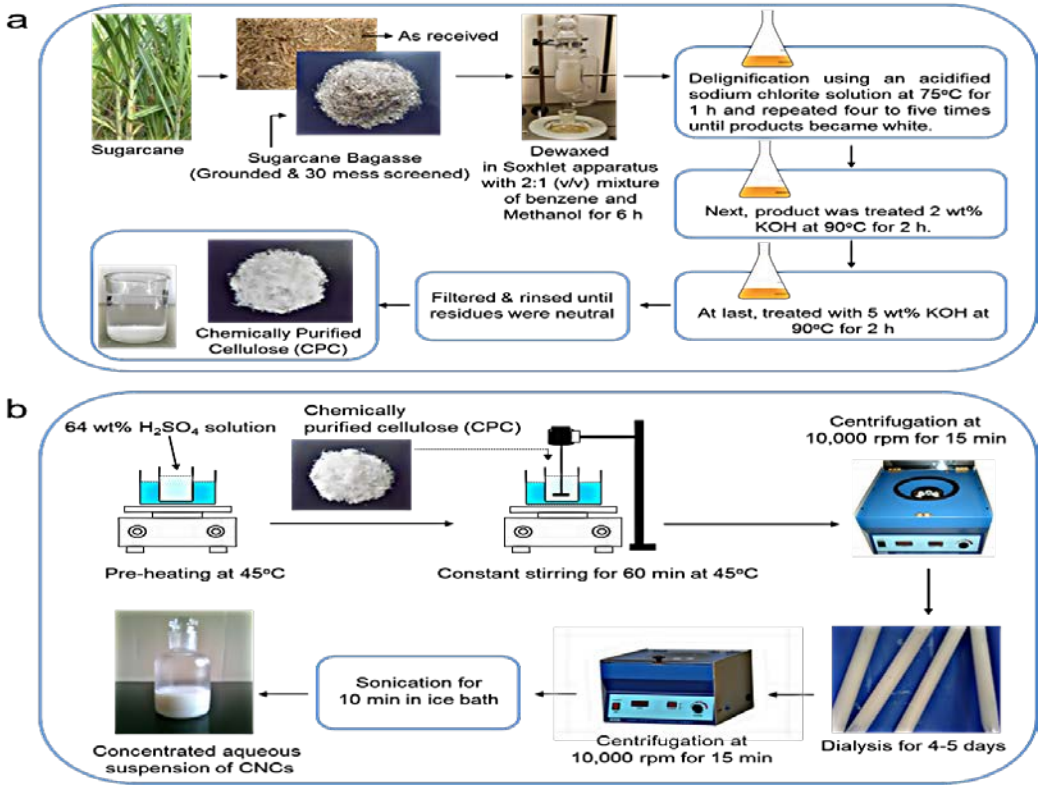

Figure 1. Schematic representation of chemical treatments: (a) Isolation of chemically purified cellulose (CPC) from sugarcane bagasse; (b) Extraction of cellulose nanocrystals (CNCs) from chemically purified cellulose (CPC)

2.2.2. Extraction of Cellulose Nanocrystals

Produced CPC was then used to extract CNCs by acid-hydrolysis as described in literature [25,38]. In brief, the hydrolysis was performed with H_2SO_4 solution (64% (w/w), 1:10 g/ml (cellulose: dilute H_2SO_4)) at 45°C for 60 min under vigorous and constant mechanical stirring. The hydrolysis reaction was quenched by adding excess (10-fold) chilled distilled water followed by successive centrifugation at 10,000-12,000 rpm for 15 min to remove acidic solution. Then sediment was collected, re-suspended in distilled water and dialyzed against distilled water until neutrality (pH 6-7). After this dialysis process, the sample was again centrifuged followed by sonication for 10 min in an ice bath to avoid overheating. Aqueous suspension thus produced was stored in refrigerator at 4°C for further use. The schematic presentation of whole process is shown in Figure 1 (b).

2.3. Characterization Methods

2.3.1. Field Emission Scanning Electron Microscopy (FE-SEM)

The surface morphology of cellulosic fibres and CNCs was examined using field emission scanning electron microscopy (FE-SEM) (FEI Quanta 200 F, Netherland) microscope with an accelerating voltage of 15–20 kV. Images showing surface morphologies of the cellulose fibres and nanocrystals were taken at various magnifications. Before examination, a fine layer of gold was sprayed on samples by an ion sputter coater with a low deposition rate. Energy dispersive x-ray (EDX) diffraction attached with FE-SEM unit was used for elemental analysis of CNCs.

2.3.2. Atomic Force Microscopy (AFM)

The topography and morphology of the CNCs were imaged using an AFM (NT-MDT NTEGRA-Multimode Scanning Probe Microscope (SPM)). Prior to imaging, a droplet of the aqueous suspension was initially dried on a glass-slide and the scans were obtained in semi-contact mode in the air.

2.3.3. Transmission Electron Microscopy (TEM)

Transmission electron microscopy (TEM) (TECNAI G^2 20 S-TWIN) was used to determine the morphology and dimensions of the CNCs obtained from the SCB cellulose fibres. A drop of a dilute aqueous suspension (0.1 wt%) was deposited on the surface of a copper grid coated with a thin carbon film. The sample was dried before TEM analysis which was carried out with an accelerating voltage of 100-120 kV.

2.3.4. Fourier Transform Infra-red (FTIR) Spectroscopy

FTIR is a fascinating technique to evaluate structural variations on samples due to the chemical treatments. The structural changes from SCB to CNCs were investigated by FTIR spectroscopy using a Nexus Thermo FTIR (ThermoNicolet, USA) spectrophotometer. The samples were oven dried at 105°C for 4-5 h, mixed with KBr in a ratio of 1:200 (w/w) and pressed under vacuum to form pellets. The FTIR spectrum of the samples was recorded in the transmittance mode in the range of 4000-500 cm^{-1}.

2.3.5. X-ray Diffraction (XRD)

The structural (physical) analysis of the samples was evaluated by X-ray diffraction (XRD) using a (Bruker AXS D8 Advance) diffractometer with a scanning rate of 5°C per min with Cu Kα radiation source (λ = 1.54060 Å) operating at 40 kV and 30 mA. The XRD patterns were obtained over the angular range 2θ = 5–60°. The Scherrer equation was used to calculate the crystal size t (nm) of cellulose I structure in respect of (200) plane:

$$Crystal\ Size\ (t) = \frac{K\lambda}{\beta_{1/2}\cos\theta}$$

Where K is the correction factor and usually taken to be 0.91, λ is the radiation wavelength, θ is the diffraction angle, and $\beta_{1/2}$ is the corrected angular width (in radians) at half maximum intensity.

2.3.6. Thermal Analysis

TG (thermogravimetry), DTG (derivative thermogravimetry) and DTA (differential thermal analysis) were carried out simultaneously by using EXSTAR TG/DTA 6300 thermogravimetric analyzer. The resolution of this instrument is 0.02μg as a function of temperature. Runs were carried out at heating rates 10°C min^{-1} from ambient temperature to 900°C (however 600°C shown in figures) under high purity nitrogen at a flow rate of 200ml min^{-1}.Thermal analysis techniques such as thermogravimetry (TG), derivative thermogravimetry (DTG) and differential thermal analysis (DTA) were widely used to measure the thermal stability and pyrolysis behavior of polymers in different conditions.

2.3.7. Image Analysis

The dimensions of the CNCs from three different images (50 nanocrystals) were measured by using ImageJ software (ImageJ 1.46, National Institute of Health (NIH), USA) by image analysis.

3. Results and Discussion

Figure 2 shows that the FE-SEM micrographs of the as received ground (30 mess screen) SCB fibres having surface layers of a high percentage of extractives (waxes, pectin, oil etc.) Figure 2a, the de-lignified SCB with cleaner surface which confirms removal of lignin with some other extractives after de-lignification with acidified sodium chlorite Figure 2b and the CPC fibrils after the removal of hemicellulose with other residual extractives due to alkali treatment Figure 2c [19] and finally the CNCs extracted by acid-hydrolysis of the CPC fibres (as shown in Figure 3a).

Here, diameter and size of fibrils of purified cellulose was reduced to great extent due to removal of all amorphous region of semi-crystalline cellulose leaving nano-scale rod-like crystals. Figure 2c clearly shows the presence of fibres which are not seen in Figure 2a and 2b.

Figure 3(b) and 3(c) show the TEM and AFM micrographs of a very dilute suspension of CNCs showing agglomerated ‘rod-like’ nanocrystals. The diameter of nanocrystals has wide range of distribution but the size of most of the ‘rod-like’ nanocrystals lies within the range 250-480 nm in length and 20-60 nm in diameter. Their

compact agglomeration of CNCs shows that cellulose chains have an intermolecular hydrogen bonding and a strong hydrophilic interaction in between the cellulosic chains.

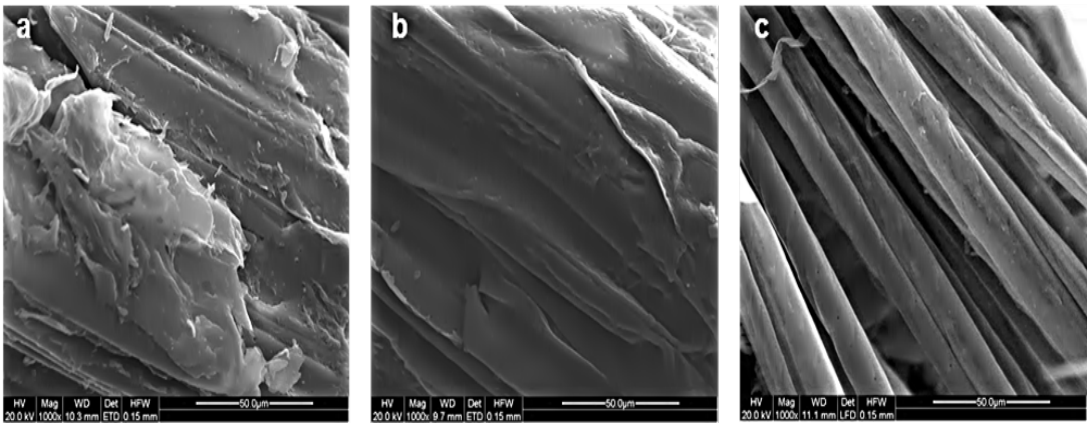

Figure 2. FE-SEM images of (a) sugarcane bagasse as raw-material; (b) de-lignified sugarcane bagasse; (c) chemically purified cellulose fibres

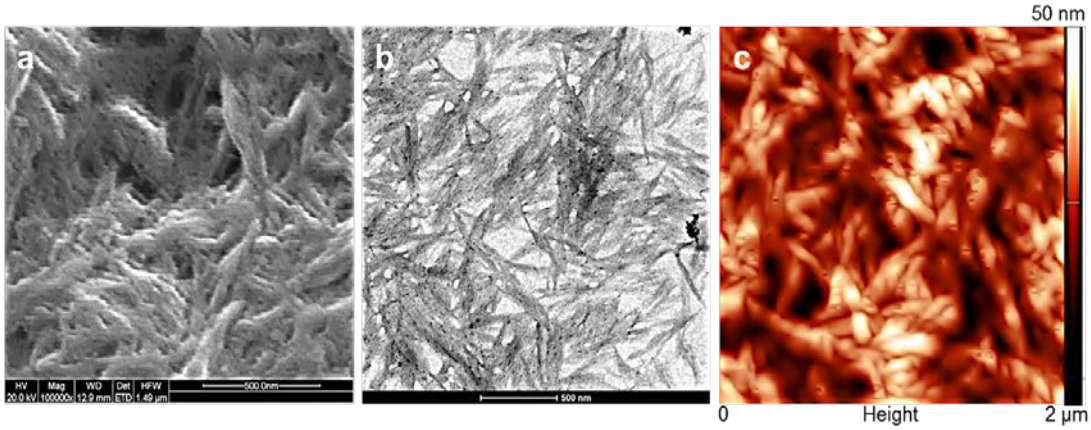

Figure 3. Morphology and topography of cellulose nanocrystals: (a) field emission-scanning electron micrograph (FE-SEM, 500 nm scale); (b) transmission electron microscopy image (TEM, 500 nm); (c) Atomic Force Microscopy (AFM, 2 µm scale)

Energy dispersive x-ray diffraction (EDX) attached with FE-SEM was used for elemental analysis of CNCs. The EDX spectrum (as shown in Figure 4) showed the peaks for carbon, oxygen and sulfur corresponding to their binding energies, respectively. CNCs contain 0.72 wt% elemental impurity of sulfur along with the main components such as carbon (43.13%) and oxygen (56.12%) as shown in Table 1. This elemental impurity is due to the acid (H_2SO_4) hydrolysis of cellulose fibres and remaining after dialysis of CNCs having sulfate groups to some extent.

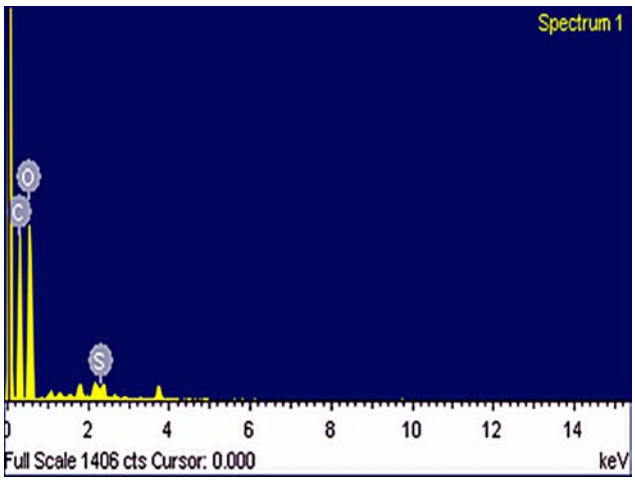

Figure 4. Energy-dispersive x-ray diffraction (EDX) spectrum of cellulose nanocrystals

Table 1. Elemental compositions of cellulose nanocrystals obtained by EDX

Element	Weight (%)	Atomic (%)
C K	43.17	50.45
O K	56.12	49.24
S K	0.72	0.31
Total	100.00	

Direct information about changes in chemical functionality can be obtained by FTIR spectroscopy which has been extensively used for structural analysis of the material before and after chemical treatments. FTIR spectra of SCB as raw material, CPC and the CNCs obtained by acid-hydrolysis are shown in Figure 5.

The spectral bands at 3175-3490 cm^{-1} (O-H stretching intramolecular hydrogen bonds for cellulose I), 2850-2970 cm^{-1} (C-H stretching), 1730 cm^{-1} (C-O stretching vibration for the acetyl and ester linkages in lignin, hemicellulose, pectin etc.), 1620-1649, 1512, and 1595 cm^{-1} (associated with the aromatic ring present in lignin and absorbed water), 1250 cm^{-1} (C–O out of plane stretching due to the aryl group in lignin), which are associated with the SCB before the chemical treatments. After chemical treatment with acidified sodium chlorite and alkali treatment, these bands are not observed in the FTIR spectrum of CPC. The effect of this chemical purification can be observed through main spectral bands which must be emphasized at 1512 and 1250 cm^{-1}. The band at 1512 cm^{-1} is absent and the band at 1250 cm^{-1} is reduced drastically in the FTIR spectrum of CPC [19,39,40,41,42].

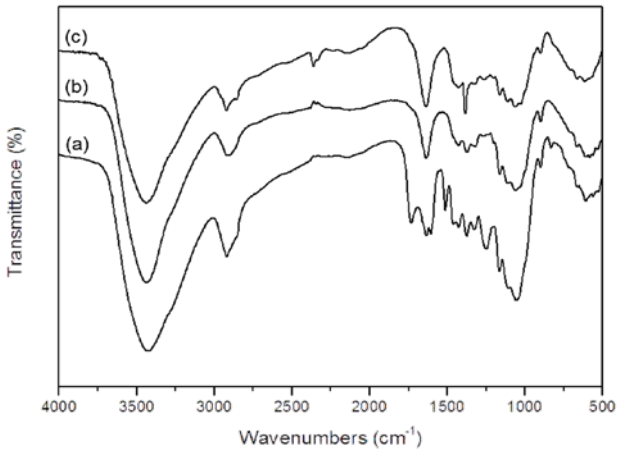

Figure 5. FTIR spectra of (a) sugarcane bagasse as raw material; (b) chemically purified cellulose; and (c) cellulose nanocrystals

However, FTIR spectra of CNCs having sharp bands but similar to that observed in CPC. The spectral band observed in the spectra of CPC and CNCs in the region 1649–1634 cm^{-1} are due to the O–H bending due to adsorbed water [40], 1430-1420 cm^{-1} is due to CH_2 scissoring motion in cellulose), 1382-1375 cm^{-1} (C-H bending), 1336 (O-H in plane bending) 1317 cm^{-1} (CH_2 wagging), 1054 cm^{-1} (C–O–C pyranose ring stretching vibration), 902-893 cm^{-1} (associated with the cellulosic β-glycosidic linkages), ~1155 cm^{-1} (C–C ring stretching band) , and at 1105 cm^{-1} (the C–O–C glycosidic ether band) [30,42,43,44]. The spectral bands observed at 1427 cm^{-1} and 897 cm^{-1} shows significant cellulose I content. In case of CNCs, spectral band at 1375 cm^{-1} was very strong while spectral band at 1335, 1315 cm^{-1} overlap and diffused and other spectral band 1278-1285 cm^{-1} is weak and diffused. On comparing these spectral data which revealed that CNCs are composed of crystalline cellulose I while content of amorphous cellulose is negligible.

These FTIR spectral peaks can be applied to analysis of crystallinity of the samples consisting cellulose I or Cellulose II or mixture of both components, and amorphous cellulose [45]. According to ref. [46] 850-1500 cm^{-1} region is sensitive to crystal structure of the cellulosic material. Spectral bands at 1420-1430 cm^{-1} and 893-897 cm^{-1} are very important to elucidate to the crystal structure of cellulosic material and its (1420/893 cm^{-1}) spectral ratio and (1375/2900 cm^{-1}) spectral ratio show index of crystallinity [46] or lateral order index (LOI) [47] and total crystallinity index (TCI) [43,44], respectively. In cellulosic samples, the spectral ratio (1430/897 cm^{-1}) gives the evidence of containing cellulose I fraction [48].

Higher value of the given index (LOI, TCI) reveals that the given material contains a highly crystalline and an ordered structure [49]. For these index values, the (1430/897 cm^{-1}) spectral ratio is low in case of CPC as compared to SCB due to chemical treatments which possibly disturbed the order of the structure to some extent and in case of CNCs increased to higher value due to removal of amorphous cellulose while the (1375/2900 cm^{-1}) spectral ratio increased from SCB to CPC to CNCs (very high values in case of CNCs).

The XRD diffraction pattern of SCB as raw material, CPC, and CNCs are shown in Figure 6.

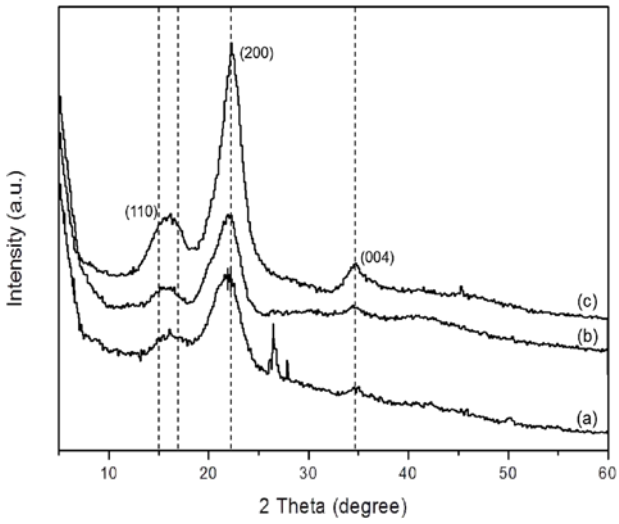

Figure 6. X-ray diffractograms of (a) sugarcane bagasse as raw material; (b) chemically purified cellulose; (c) cellulose nanocrystals produced by acid-hydrolysis from chemically purified cellulose

These samples exhibited a peak around $2\theta = 16.5^{o}$ and 22.5^{o} and 34.6^{o} which are supposed to represent the typical cellulose-I structure. The cellulose crystals exhibit characteristic assignments of 110, 200, and 004 planes, respectively [19,37,50]. The crystallinity index of the samples was calculated according to amorphous subtraction method [51]. The crystallinity index of the SCB was calculated as 35.6% and increased in case of CPC to 63.5% (due to removal of lignin and hemicelluloses as amorphous part) [19], and 72.5% in case of CNCs in which remaining amorphous part was removed during acid-hydrolysis. These results of crystallinity degree from XRD analysis follow the similar trend as results calculated by crystallinity analysis from FTIR spectra. Crystallite size of CPC fibres and CNCs was calculated 4.2 nm and 3.5 nm, respectively (as shown in Table 2).

Table 2. FTIR and XRD analysis parameters for Calculated Lateral Order Index (LOI), total crystallinity index (TCI), crystallinity percentage and crystal size

Sample	Lateral Order Index (LOI) (1430/897 cm^{-1})	Total Crystallinity Index (TCI) (1375/2900 cm^{-1})	Crystallinity (%)	Crystal Size (nm) in respect to the (200) planes
Sugarcane Bagasse (SCB)	0.4990 ± 0.0132	0.3552 ± 0.0210	35.6	--
Chemically Purified Cellulose (CPC)	0.3630 ± 0.0270	0.4683 ± 0.0133	63.5	4.2
Cellulose Nanocrystals (CNCs)	0.5744 ± 0.0023	1.3231 ± 0.0152	72.5	3.5

The study of thermal properties (TG-DTG-DTA) of materials is a dynamic phenomenological approach to investigate the response to a change in temperature. TG curves show only changes in weight during heating and its derivative shows changes in the TG slope which may not be obvious from the curve of TG. The DTA curves show the difference in temperature as exothermic or endothermic reactions in a sample. Figure 7 (a and b) and

Figure 8 demonstrate the investigation of thermal properties of SCB as raw material, CPC, and CNCs extracted by acid-hydrolysis.

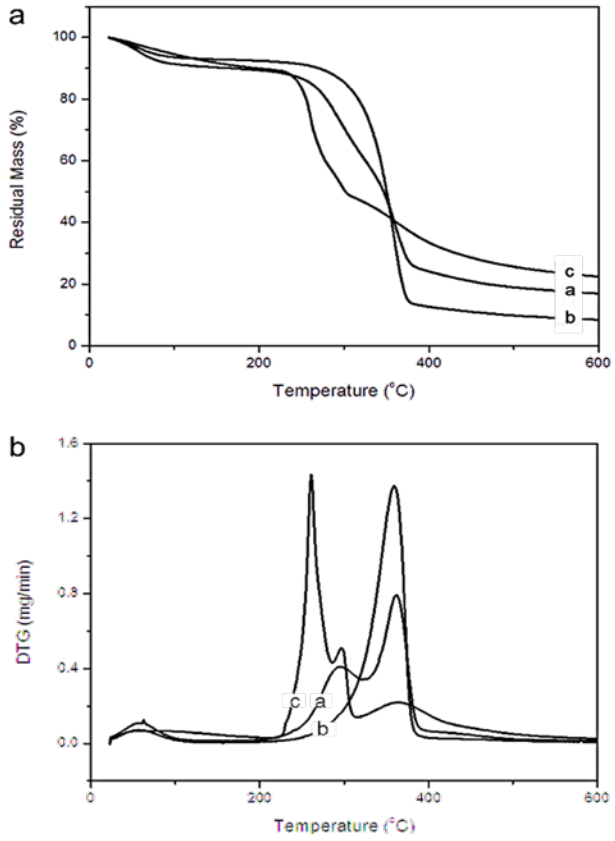

Figure 7. Thermal analysis of sugarcane bagasse, chemically purified cellulose, and Cellulose nanocrystals (A) TG curve; (B) DTG curve

As can be seen, the initial mass losses starting at ~25°C for both SCB and CPC and at 32°C for CNCs (due to high solvation capacity with water molecule) showing evaporation of loose surface bound moisture (H_2O). The intermolecularly H-bonded water is evaporated at near about 120°C for all three samples. The degradation of SCB starts forward at 270°C and the rate of degradation reaches its peak at 363 °C (observed by DTG curve) while that of CPC occurs at 288°C and the rate of degradation becomes maximum at 360°C (observed by DTG curve). The degradation of CNCs occurs afterward at 236°C, showing additional small shoulder and rate of degradation is reached at 300°C (also observed by DTG curve).

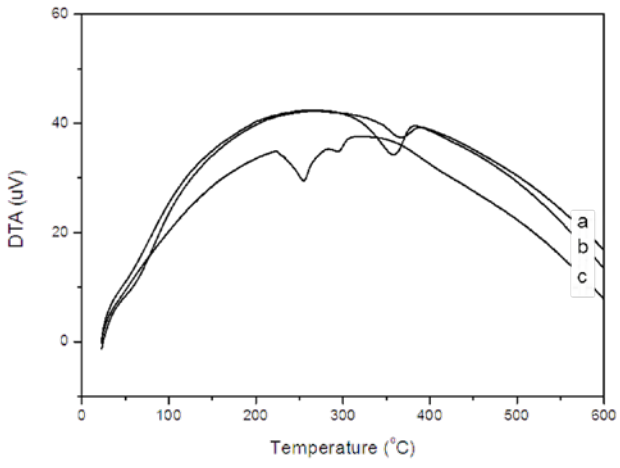

Figure 8. DTA curves of sugarcane bagasse, chemically purified cellulose, and Cellulose nanocrystals

Low degradation temperature of SCB than that of CPC is due to the presence of lignin, hemicelluloses and other non-cellulosic segment which decompose at low temperature. Generally, cellulose thermal degradation involves dehydration, depolymerisation and decomposition of glycosyl-units and then formation of a charred residue. In case of CNCs, thermal degradation occurs at a lower temperature within broader ranges of temperature showing lower thermal stability due to their nano-sizes, greater number of free ends in the chain of CNCs, and may show drastic reduction in the molecular weight and degradation of highly sulfated amorphous regions [30]. In TG curve, acid-hydrolyzed CNCs showed mainly two humps or shoulder in close proximity where lower degradation temperature may correspond to highly sulfated amorphous regions and higher degradation temperature correspond to unsulfated part of the material [52]. DTG curve shows degradation of CNCs in three process of pyrolysis (two well separated pyrolysis process [53] mainly at 220-270°C, 270-330°C, and 330-470°C, respectively [54] and maximum temperature peak (DTG curve) occurred at a much lower temperature than the degradation temperature (around 400°C) of native cellulose [55]. Here, remnant sulfate groups are responsible for the reduced thermal-stability of the nanocrystals [52] because the elimination of H_2SO_4 in sulfated anhydro-glucose units require less energy [56], therefore, sulfuric acid molecules were released at much lower temperatures during the degradation process.

The char formation of CNCs is the highest in these three materials where char formation of SCB (13.51%) is higher than that of CPC (5.81%). Actually, bagasse contains high amount of cellulose-I (having parallel orientation) other than low-temperature degrading materials (such as lignin, hemicellulose etc.) while CPC contains high amount of crystalline cellulose-I and amorphous cellulose and in case of CNCs, content of cellulose I is higher while amorphous cellulose hydrolyzed. Larger amount of char formation of CNCs (17.36%) may be because of three basic reasons: (1) Due to nano-size and greater number of the free ends of the chains of CNCs which decompose at a lower temperature; (2) H_2SO_4 (a dehydrating agent) which facilitate the depolymerisation or decomposition of cellulose by removing some of the -OH groups either by direct catalysis or mechanism of esterification [57,58] and presence of H^+ ion (around pH 5.5-6) promote increased formation of char residue because of removal of oxygen in the form of H_2O which prevent weight losses; (3) highly crystalline nature (cellulose crystal) of CNCs increase the proportion of carbon, therefore formation of char residue increased as carbon content increases [50,58].

DTA traces of SCB, CPC, and CNCs show two distinct endothermic changes (as shown in Figure 8) depending on the composition of the material. First endotherm occurs at much lower than 100°C due to the loss of moisture evaporation (as described in TG thermograms). Second endotherm is an indication of the process of fusion or melting of crystallites showing nature of decomposition. The course of evaporation depends mainly on variation in holding capacity of moisture by the sorptive forces due to constituents. In case of bagasse, there is variation in holding capacity due to lignin, hemicellulose, and other non-cellulosic materials showing loss of moisture in a

wider range of temperature while purified cellulose involved in relatively uniform sorptive forces causing loss of moisture within a narrow temperature range. In case of CNCs, sulfuric acid behaves as a dehydrating agent and sulfated groups reduce the affinity towards moisture absorption. Therefore, small quantity of moisture absorbed on surface of CNCs and at much lower temperature it evaporated off from surface. The fusion or melting process of SCB occurs over a wider range of temperature because of different constituents which have their own characteristic melting regions produced [30]. After removal of lignin, hemicellulose and other non-cellulosic materials, chemical treatment, CPC is of more compact crystals structure which gives higher onset temperature of crystal melting with narrow endotherm width in turn (255-295°C). In case of acid-hydrolyzed CNCs, all amorphous regions were dissolved and only nano-scale cellulose crystals having sulfated hydroxyl (-OH) groups and gives higher onset temperature of crystal melting with wider endotherm width in turn (220-380°C).

4. Conclusions

Sugarcane bagasse (SCB) can be utilized as source of cellulose for producing CNCs. The preparation of CNCs was done in two steps of chemical treatments by chemical purification and acid-hydrolysis. The chemical purification process through acidic sodium chlorite and alkali treatment gives the white coloured chemically purified cellulose which was further acid-hydrolyzed to extract CNCs. The morphology and topography of the nanocrystals were characterized by FE-SEM, TEM and AFM. FE-SEM and AFM studies which showed supporting evidence with TEM analysis for CNCs of nano-scale range. The CNCs were with average size of 'rod-like' nanocrystals ranging from 250-480 nm for length and 20-60 nm for diameter. Elemental analysis (EDX) showed 0.72 wt% sulfur impurity in CNCs alongwith other main components. The structural changes were measured by FTIR and XRD, and thermal analysis was measured by TG-DTG-DTA which revealed that CNCs showed lower thermal stability and higher crystallinity (72.5%) as compared to native cellulose (63.5%). This investigation shows that this chemical approach may be promisingly very efficient process for the preparation of CNCs from SCB.

Acknowledgement

The authors are thankful to the Ministry of Human Resource Development (MHRD), New Delhi for providing financial support to one of the authors Mr. Anuj Kumar and Indian Institute of Technology Roorkee (IIT Roorkee) for various other infrastructures required for the advanced research work in the field of biocomposites.

References

[1] Faruka, O., Bledzki, A. K., Fink, H. P., and Sain, M., "Biocomposites reinforced with natural fibers: 2000-2010". *Prog. Polym. Sci.*, 37, 1552-1596, 2012.

[2] Vartiainen, J., Pohler, T., Sirola, K., Pylkkanen, L., Alenius, H., Hokkinen, J., Tapper, U., Lahtinen, P., Kapanen, A., Putkisto, K., Hiekkataipale, P., Eronen, P., Ruokolainen, J., and Laukkanen, A., "Health and environmental safety aspects of friction grinding and spray drying of microfibrillated cellulose", *Cellulose*, 18, 775-786, 2011.

[3] Lin, N., Huang, J., and Dufresne, A., "Preparation, properties and applications of polysaccharide nanocrystals in advanced functional nanomaterials: a review", *Nanoscale*, 4, 3274-3294, 2012.

[4] Lavoine, N., Desloges, I., Dufresne, A., and J. Bras, J., "Microfibrillated cellulose - Its barrier properties and applications in cellulosic materials: A review", *Carbohydr. Polym.*, 90:735-764, 2012.

[5] Habibi, Y., Lucia, L.A., and O. J. Rojas, O. J., "Cellulose Nanocrystals: Chemistry, Self-Assembly, and Applications", *Chem. Rev.*, 110, 3479-3500, 2010.

[6] Moon, R.J., Martini, A., Nairn, J., Simonsen, J., and Youngblood, J., "Cellulose nanomaterials review: structure, properties and nanocomposites", *Chem. Soc. Rev.*, 40, 3941-3994, 2011.

[7] Klemm, D., Kramer, F., Moritz, S., Lindstrom, T., Ankerfors, M., Gray, D., and Dorris, A., "Nanocelluloses: A New Family of Nature-Based Materials", *Angew. Chem. Int. Ed.*, 50, 5438-5466, 2011.

[8] Hu, L., Zheng, G., Yao, J., Liu, N., Weil, B., Eskilsson, M., Karabulut, E., Ruan, Z., Fan, S., Jason, T., Bloking, J. T., McGehee, M.D., Wågberg, L., and Cui. Y., "Transparent and conductive paper from nanocellulose fibers", *Energy Environ. Sci.*, 6, 513-518, 2013.

[9] Siro, I., and D. Plackett, D., "Microfibrillated cellulose and new nanocomposite materials: a review", *Cellulose*, 17, 459-494, 2010.

[10] Podsiadlo, P., Choi, S., Shim, B., Lee, J., Cuddihy, M., and Kotov, N. A., "Molecularly engineered nanocomposites: layer-by-layer assembly of cellulose nanocrystals", *Biomacromolecules*, 6, 2914-2918, 2005.

[11] Fortunati, E., Puglia, D., Monti, M., Peponi, L., Santulli, C., Kenny, J.M., and Torre, L., "Extraction of Cellulose Nanocrystals from Phormium tenax Fibres", *J. Polym. Environ*, 21, 319-328, 2013.

[12] Siqueira, G., Tapin-Lingua, S., Bras, J., da Silva Perez, D., and Dufresne, A., "Mechanical properties of natural rubber nanocomposites reinforced with cellulosic nanoparticles obtained from combined mechanical shearing, and enzymatic and acid hydrolysis of sisal fibers", *Cellulose*, 18, 57-65, 2010.

[13] Dong, H., Snyder, J. F., Tran, D.T., and Leadore, J. L., "Hydrogel, aerogel and film of cellulose nanofibrils functionalized with silver nanoparticles", *Carbohydr. Polym*, 95, 760-767, 2013.

[14] Zhou, Y., Fuentes-Hernandez, C., Khan, T. M., Liu, J.C., Hsu, J., Shim, J. W., Dindar, A., Youngblood, J.P., Moon, R.J., and Kippelen, B., "Recyclable organic solar cells on cellulose nanocrystal substrates", *Sci. Rep.*, 3, 1-5, 2013.

[15] Azizi Samir, M. A. S., Alloin, F., and Dufresne, A., "Review of recent research into cellulosic whiskers, their properties and their application in nanocomposite field", *Biomacromolecules*, 6, 612-626, 2005.

[16] Eichhorn, S. J., Dufresne, A., Aranguren, M., Marcovich, N.E., Capadona, J. R., Rowan, S. J., Weder, C., Thielemans, W., Roman, M., Renneckar, S., Gindl, W., Veigel, S., Keckes, J., Yano, H., Abe, K., Nogi, M., Nakagaito, A.N., Mangalam, A., Simonsen, J., Benight, A. S., Bismarck, A., Berglund, L.A., and Peijs, T., "Review: Current international research into cellulose nanofibres and nanocomposites", *J. Mater. Sci.*, 45, 1-33, 2010.

[17] Sheltami, R.M., Abdullah, I., Ahmad, I., Dufresne, A., and Kargarzadeh, H., "Extraction of cellulose nanocrystals from mengkuang leaves (Pandanus tectorius)", *Carbohydr. Polym*, 88, 772- 779, 2012.

[18] Johar, N., Ahmada, I., and Dufresne, A., "Extraction, preparation and characterization of cellulose fibres and nanocrystals from rice husk", *Indus. Crop. Prod.*, 37, 93-99, 2012.

[19] Kumar, A., Negi, Y.S., Bhardwaj, N.K., and Choudhary, V., "Synthesis and characterization of methylcellulose/PVA based porous composite", *Carbohydr. Polym*, 88, 1364-1372, 2012.

[20] Neto, W. P. F., Silvério, H. A., Dantas, N. O., and Pasquini, D., "Extraction and characterization of cellulose nanocrystals from agro-industrial residue - Soy hulls", *Indus. Crop. Prod.*, 42, 480-488, 2013.

[21] Silvérioa, H. A., Neto, W. P. F., Dantas, N. O., and Pasquini, D., "Extraction and characterization of cellulose nanocrystals from corncob for application as reinforcing agent in nanocomposites", *Indus. Crop. Prod.*, 44, 427-436, 2013.

[22] Pasquini, D., Teixeira, E. D. M., Curvelo, A. A. D.S., Belgacem, M. N., and Dufresne, A., "Extraction of cellulose whiskers from

cassava bagasse and their applications as reinforcing agent in natural rubber", *Indus. Crop. Prod.*, 32, 486-490, 2010.

[23] Zuluaga, R., Putaux, J. L., Cruz, J., Velez, J., Mondragon, I., and Ganan, P., "Cellulose microfibrils from banana rachis: effect of alkaline treatment on structural and morphological features", *Carbohydr. Polym*, 76, 51-59, 2009.

[24] Wong, S., and Shanks, R., *Biocomposites of natural fibers and poly (3-hydroxybutyrate) and copolymers: Improved mechanical properties through compatibilization at the interface*. In L. Yu (Ed.), Biodegradable polymer blends and composites from renewable resources, New Jersey: John Wiley & Sons, Inc. 2009 303-347.

[25] Beck-Candanedo, S., Roman, M., and Gray, D. G., "Effect of reaction conditions on the properties and behavior of wood cellulose nanocrystal suspensions", *Biomacromolecules*, 6, 1048-1054, 2005.

[26] Pandey, J. K., Ahn, S. H., Lee, C. S., Mohanty, A. K., and Misra, M., "Recent advances in the application of natural fiber based composites", *Macromol. Mater. Eng.*, 295, 975-989, 2010.

[27] Deepa, B., Abraham, E., Cherian, B. M., Bismarck, A., Blaker, J. J., Pothan, L.A., Leao, A. L., de Souza, S.F., and Kottaisamy, M., "Structure, morphology and thermal characteristics of banana nano fibers obtained by steam explosion", *Biores. Technol.*, 102, 1988-1997, 2011.

[28] Peng, B. L., Dhar, N., Liu, H.L., and Tam, K. C., "Chemistry and applications of nanocrystalline cellulose and its derivatives: a nanotechnology perspective", *Can. J. Chem. Eng.*, 89, 1191-1206, 2011.

[29] Li, J., Wei, X., Wang, Q., Chen, J., Chang, G., Kong, L., Su, J., and Liu, Y., "Homogeneous isolation of nanocellulose from sugarcane bagasse by high pressure homogenization", *Carbohydr. Polym*, 90, 1609-1613, 2012.

[30] Mandal, A., and Chakrabarty, D., "Isolation of nanocellulose from waste sugarcane bagasse (SCB) and its characterization", *Carbohydr. Polym*, 86, 1291-1299, 2011.

[31] Teixeira, E.de M., Bondancia, T.J., Teodoro, K. B. R., Correa, A. C., Marconcini, J. M., and Mattoso, L. H. C., "Sugarcane bagasse whiskers: Extraction and characterizations", *Indus. Crop. Prod.*, 33, 63-66, 2011.

[32] Bhattacharya, D., Germinario, L. T. Winter, W. T., "Isolation, preparation and characterization of cellulose microfibers obtained from bagasse", *Carbohydr. Polym*, 73, 371-377, 2008.

[33] Kumar, A., Negi, Y. S., Bhardwaj, N. K., and Choudhary, V., "Synthesis and characterization of cellulose nanocrystals/PVA based bionanocomposite", *Adv. Mater. Lett*, 4, 626-631, 2013.

[34] Maddahy, N. K., Ramezani, O., and Kermanian, H., *Production of Nanocrystalline Cellulose from Sugarcane Bagasse*, Proceedings of the 4th International Conference on Nanostructures (ICNS4) 12-14 March, Kish Island, I. R. Iran, 2012.

[35] Abe, K., Iwamoto, S., and Yano, H., "Obtaining cellulose nanofibres with a uniform width of 15 nm from wood", *Biomacromolecules*, 8, 3276-3278, 2007.

[36] Abe, K., and Yano, H., "Comparison of the characteristics of cellulose microfibril aggregates of wood, rice straw, and potato tuber", *Cellulose* 16, 1017-1023, 2009.

[37] Chen, W. S., Yu, H. P., Liu, Y. X., Chen, P., Zhang, M. X., and Hai, Y. F., "Individualization of cellulose nanofibres from wood using high-intensity ultrasonication combined with chemical pretreatments", *Carbohydr. Polym*, 83, 1804-1811, 2011.

[38] Bondeson, D., Mathew, A., and Oksman, K., "Optimization of the isolation of nanocrystals from microcrystalline cellulose by acid hydrolysis", *Cellulose*, 13, 171 -180, 2006.

[39] Viera, R. G. P., Filho, G. R., de Assuncao, R. M. N., Meireles, C. S., Vieira, J. G., and de Oliveira, G. S., "Synthesis and characterization of methylcellulose from sugarcane bagasse cellulose", *Carbohydr. Polym*, 67, 182-189, 2007.

[40] Troedec, M., Sedan, D., Peyratout, C., Bonnet, J., Smith, A., Guinebretiere, R., Gloaguen, V., and Krausz, P., "Influence of various chemical treatments on the composition and structure of hemp fibers", *Composites Part A-Appl. Sci. Manufact.*, 39, 514-522, 2008.

[41] Sain, M., and Panthapulakkal, S., "Bioprocess preparation of wheat straw fibers and their characterization", *Indus. Crop. Prod.*, 23, 1-8, 2006.

[42] Garside, P., and Wyeth, P., "Identification of cellulosic fibres by FTIR spectroscopy: Thread and single fibre analysis by attenuated total reflectance", *Stud. Conser*, 48, 269-275, 2003.

[43] Nelson, M. L., and O'Connor, R. T., "Relation of certain infrared bands to cellulose crystallinity and crystal lattice type. Part I. Spectra of lattice types I, II, III and amorphous cellulose", *J. Appl. Polym. Sci.*, 8, 1311-1324, 1964.

[44] Nelson, M. L., and O'Connor, R. T., "Relation of certain infrared bands to cellulose crystallinity and crystal lattice type. Part II. A new infrared ratio for estimation of crystallinity in cellulose I and II", *J. Appl. Polym. Sci.*, 8, 1325-1341, 1964.

[45] Carrillo, F., Colom, X., Sunol, J. J., and Saurina, J., "Structural FTIR analysis and thermal characterization of lyocell and viscose-type fibres", *Eur. Polym. J.*, 40, 2229-2234, 2004.

[46] O'Connor, R. T., DuPre, E. F., and Mitcham, D., "Application of infrared absorption spectroscopy to investigations of cotton and modified cottons. Part 1: physical and crystalline modifications and oxidation", *Textile Res. J.*, 28, 382-392, 1958.

[47] Hurtubise, F. G., and Krassig, H., "Classification of fine structural characteristics in cellulose by infrared spectroscopy. Use of potassium bromide pellet technique", *Anal. Chem.*, 32, 177-181, 1960.

[48] Oh, S. Y., Dong, I. Y., Shin, Y., Hwan, C. K., Hak, Y. K., Yong, S.C., Won, H. P., and Ji. H. Y., "Crystalline structure analysis of cellulose treated with sodium hydroxide and carbon dioxide by means of X-ray diffraction and FTIR spectroscopy", *Carbohydr. Res.*, 340, 2376-2391, 2005.

[49] Spiridon, I., Teaca, C.A., and Bodirlau, R., "Structural changes evidenced by FTIR Spectroscopy in cellulosic materials after pretreatment with ionic-liquid and enzymatic hydrolysis", *Bioresources*, 6, 400-413, 2010.

[50] Wada, M., Heux, L., and Sugiyama, J., "Polymorphism of cellulose I family: Reinvestigation of cellulose IV", *Biomacromolecules*, 5, 1385-1391, 2004.

[51] Park, S., JBaker, J. O., Himmel, M.E., Parilla, P.A., and Johnson, D. K., "Cellulose crystallinity index: Measurement techniques and their impact on interpreting cellulase performance", *Biotechnol. Biofuels*, 3, 1-10, 2010.

[52] Maren, R., and William, T. W., "Effect of sulfate groups from sulfuric acid hydrolysis on the thermal degradation behavior of bacterial cellulose", *Biomacromolecules*, 5, 1671-1677, 2004.

[53] Wang, N., Ding, E. Y., Chang, R. S., "Thermal degradation behaviors of spherical cellulose nanocrystals with sulfate groups", *Polymer*, 48, 3486-3493, 2007.

[54] Li, W., Wang, R., and Liu, S., "Nanocrystalline cellulose prepared from softwood kraft pulp via ultrasonic-assisted acid hydrolysis", *Bioresources*, 6, 4271-4281, 2011.

[55] George. J., Sajeevkumar, V.A., Kumar, R., Ramana, K. V., Sabapathy, S. N., and Bawa, A. S., "Enhancement of thermal stability associated with the chemical treatment of bacterial (Gluconacetobacter xylinus) cellulose", *J. Appl. Polym. Sci.*, 8, 1845-1851, 2008.

[56] Julien, S., Chornet, E., and Overand, R. P., "Influence of acid pretreatment (H_2SO_4, HCl, HNO_3) on reaction selectivity in the vacuum pyrolysis of cellulose", *J. Analytic. Appl. Pyrol.*, 27, 25-43, 1993.

[57] Kim, D. Y., Nishiyama, Y., Wada, M., and Kuga, S., "High yield carbonization of cellulose by sulfuric acid impregnation", *Cellulose*, 8, 29-33, 2008.

[58] George, J., Ramana, K. V., Bawa, A. S., and Siddaramaiah, "Bacterial cellulose nanocrystals exhibiting high thermal stability and their polymer nanocomposites", *Internl. J. Biologic. Macromol*, 48, 50-57, 2011.